# MIT Libraries | DSpace@MIT

## MIT Open Access Articles

## *Broadband super-collimation in a hybrid photonic crystal structure*

**Massachusetts Institute of Technology**

# Broadband super-collimation in a hybrid photonic crystal structure

**Rafif E. Hamam, Mihai Ibanescu, Steven G. Johnson,
J. D. Joannopoulos, and Marin Soljačić**

*Center for Materials Science and Engineering and Research Laboratory of Electronics,
Massachusetts Institute of Technology, Cambridge, Massachusetts 02139, USA*

*rafif@mit.edu*

**Abstract:** We propose a photonic crystal (PhC) structure that supports super-collimation over a large frequency range (over 4 times that of a traditional square lattice of holes). We theoretically and numerically investigate the collimation mechanism in our structure, in comparison to that of two other frequently used related PhC structures. We also point out the potential importance of our proposed structure in the design of super-collimation-based devices for both monochromatic and polychromatic light.

**OCIS codes:** (350.4238) Nanophotonics and photonic crystals; (260.2110) Electromagnetic optics

---

### References and links

1. John D. Joannopoulos, Steven G. Johnson, Joshua N. Winn, and Robert D. Meade, *Photonic Crystals: Molding the Flow of Light*, second edition (Princeton University Press, 2008).
2. J. N. Winn, Y. Fink, S. Fan, and J. D. Joannopoulos, Opt. Lett. 23, pp. 1573-1575 (October 1998).
3. R. D. Meade, A. Devenyi, J. D. Joannopoulos, O. L. Alerhand, D. A. Smith, and K. Kash, J. Appl. Phys. 75, pp. 4753-4755 (May 1994).
4. S. Fan, P. R. Villeneuve, J. D. Joannopoulos, and E. F. Schubert, Phys. Rev. Lett. 78, pp. 3294-3297 (April 1997).
5. C. Luo, S. G. Johnson, and J. D. Joannopoulos, Appl. Phys. Lett. 81, pp. 2352-2354 (2002).
6. M. Soljačić and J. D. Joannopoulos, Nat. Mat. 3, pp. 211-219 (April 2004).
7. M. Soljačić, E. Lidorikis, J. D. Joannopoulos, and L. V. Hau, Appl. Phys. Lett. 86, p. 171101 (April 2005).
8. D. L. C. Chan and M. Soljačić, and J. D. Joannopoulos, Opt. Express 14, p. 8785 (September 2006).
9. Hideo Kosaka, Takayuki Kawashima, Akihisa Tomita, Masaya Notomi, Toshiaki Tamamura, Takashi Sato, and Shojiro Kawakami, Appl. Phys. Lett. 74 (9), p.p. 1212-1214 (1999).
10. Lijun Wu, Michael Mazilu, and Thomas F. Krauss, J. Lightwave Tech. 21 (2), p.p. 561-566 (February 2003).
11. Dennis W. Prather, Shouyuan Shi, David M. Pustai, Caihua Chen, Sriram Venkataraman, Ahmed Sharkawy, Garrett J. Schneider, and Janusz Murakowski, Opt. Express 29 (1), p.p. 50-52 (January 2004).
12. Jonghwa Shin and Shanhui Fan, Opt. Lett. 30 (18), p.p. 2397-2399 (September 2005).
13. Peter T. Rakich, Marcus S Dahlem, Sheila Tandon, Mihai Ibanescu, Marin Soljačić, Gale S. Petrich, John D. Joannopoulos, Leslie A. Kolodziejski and Erich P. Ippen, Nat. Mat. 5, p.p. 93-96 (February 2006).
14. Ta-Ming Shih, Andre Kurs, Marcus Dahlem, Gale Petrich, Marin Soljacic, Erich Ippen, Leslie Kolodziejski , Katherine Hall, and Morris Kesler, Appl. Phys. Lett. 93, 131111, (2008).
15. Ashcroft & Mermin, *Solid State Physics* (Saunders College, 1976).
16. Demetrios N. Christodoulides, Falk Lederer & Yaron Silberberg, Nature 424, p. 817 (August 2003).
17. Steven G. Johnson and J. D. Joannopoulos, Optics Express 8, no. 3, 173-190 (2001).
18. T. Rowan, "Functional Stability Analysis of Numerical Algorithms", Ph.D. thesis, Department of Computer Science, University of Texas at Austin, 1990.
19. C. Luo, M. Soljacic, and J. D. Joannopoulos, Superprism effect based on phase velocities, Optics Letters, vol. 29, pp. 745747, April 2004.

---

## 1. Introduction

The ability of photonic crystals (PhCs) to "mold the flow of light"[1] has resulted in a remarkable variety of fascinating optical phenomena, such as omnidirectional reflection[2], low loss bends[3], high-Q cavities[3], efficient spontaneous emission[4], negative refraction[5], enhancement of nonlinear effects[6], ultrafast all-optical switching[7], and thermal emission design[8]. Super-collimation, or diffractionless light propagation, represents an additional important property made possible by the powerful versatility of PhCs. It was first described by Kosaka et. al[9], and subsequently by several other groups[10, 11, 12, 13, 14]. In all these demonstrations of super-collimation, the nondiffractive propagation is achieved by having a flat constant-frequency contour (CFC) in the dispersion relation of the PhC. When a beam, having the same frequency as the flat CFC, propagates in the PhC normal to the direction of the flat CFC, the Fourier components of the beam propagate with group velocities pointing in almost the same direction, and hence the beam does not spread much. However, in all the earlier observations of super-collimation in PhCs, the flat feature is usually confined to a not very broad frequency range around the frequency of the flat CFC, thus limiting the bandwidth over which super-collimation can be observed, and making super-collimation sensitive to variations in the frequency of the propagating monochromatic beam. For example, super-collimation has been observed along the diagonal directions of a PhC consisting of a 2D square lattice of circular holes in a dielectric[13], a schematic of which is shown in Fig. 1a. The super-collimation property in such a structure manifests itself only in a narrow frequency interval, within which the CFC's curvature flips sign. This is depicted in Fig. 1b, where we show a typical color contour plot of the first TE (electric field in the plane of periodicity) band for the structure of Fig. 1a. The change in the sign of the CFC's curvature implies the existence of a CFC with zero curvature, thus leading to super-collimation at the frequency of that particular CFC, and in a narrow frequency range around it. This stimulates the interest to search for PhC structures that support super-collimation over a larger frequency range. The band diagram of these PhCs would consist of extended frequency ranges over which the CFCs are flat enough to substantially suppress diffraction. A hint as to how to achieve this feature can be inferred from the flatness of tight-binding bands for electrons in solids[15]. The fact that tight-binding bands arise from the weak overlap between atomic orbitals inspires us to consider the simple, well-known waveguide array structure depicted in Fig 1c. We show a typical projected band diagram for the first TM (electric field perpendicular to the plane) band for such a structure in Fig. 1d, together with a color contour plot of the first TM band in Fig. 1e. Although this structure is not commonly used for super-collimation purposes, its CFCs (in a given band) get flatter as the frequency increases. However, the curvature of these contours doesn't change sign, and hence it doesn't go through zero, which would be a conventional criterion for super-collimation. Therefore, to obtain a PhC that supports super-collimation over an extended frequency range, we consider a hybrid PhC structure that combines features from both of the above-mentioned PhC types. Namely, we propose inserting into the waveguide array structure a square lattice of circular rods having the same refractive index as the waveguides, such that the rods are placed halfway between neighboring waveguides, with a lattice constant equal to the nearest-neighbor waveguide spacing. A schematic of this hybrid structure is shown in Fig. 2a. In this manuscript, we investigate the phenomenon of super-collimation in this hybrid structure, and show how it simultaneously inherits useful properties from both of the structures in Fig. 1a and Fig. 1c: the sign flip of the CFCs' concavity (due to the discrete translational symmetry) from the 2D holes-in-dielectric structure, and the extended frequency range (over 4 times the frequency range of a traditional square lattice of holes) of the flat CFCs (due to the weakly coupled waveguides), from the waveguide array structure. More specifically, in our proposed PhC structure, the photonic modes of higher-order-bands have their energy mostly concentrated in the waveguides,

and neighboring waveguides couple weakly, thus giving rise to tight-binding-like flat bands. So, one might be tempted to think that the rods don't play any role, and consequently that the performance of our proposed structure is not very promising, given the known fact that, in linear waveguide arrays, a beam initially localized in one of the waveguides is observed to hop quickly to the other waveguides in what is known as discrete diffraction[16]. However, as we will see later in this letter, the rods play an important role; in fact, by breaking the continuous translational symmetry along the waveguides' direction, the rods place our proposed structure at an advantage over the waveguide array, since they enable the existence of a CFC with zero concavity.

## 2. Super-collimation mechanism in our proposed structure

We begin the study of super-collimation in our proposed structure by considering the fourth transverse magnetic (TM) band. Because of time-reversal symmetry, the dispersion relation is an even function of $k_y$, the $y$-component of the Bloch wavevector. For small values of $k_y$, the angular frequency is described by an expansion in terms of even powers of $k_y$, namely

$$\omega_4^{TM}(k_x, k_y) = \omega_4^{TM}(k_x, 0) + \alpha_4^{TM}(k_x) \cdot (k_y)^2 + \beta_4^{TM}(k_x) \cdot (k_y)^4 + \dots \quad (1)$$

where $\omega_4^{TM}$ denotes the angular frequency of the fourth TM band. Since we aim at the optimum super-collimation performance of our proposed structure, and since small $\alpha_4^{TM}(k_x)$ is necessary to achieve super-collimation, we search for the particular rods' radius $r$ and waveguide thickness $t$ that minimize the absolute value of $\alpha_4^{TM}(k_x)$, while we set the refractive index of both rods and waveguides to $n = 3.5$. We carried out such optimization calculations by using the MIT Photonic Bands (MPB[17, 18]) software. The values of $r$ and $t$ that give rise to flat CFCs over the largest frequency range in the fourth TM band of the proposed structure, are those that minimize the maximum (over $k_x$) of $|\alpha_4^{TM}(k_x)|$. The result of this optimization calculation for $\min_{r,t} \max_{k_x} |\alpha_4^{TM}|$ corresponds to $r = 0.16a$ and $t = 0.2a$, where $a$ is the lattice constant. We calculated the TM bands of this optimum structure, by using MPB, with a spatial resolution of 128 pixels/$a$ , and we show in Fig. 2b the projected band diagram of the lowest four TM bands. We also present in Fig. 2c a color contour plot of the fourth TM band, as a function of $k_x$ and $k_y$. We observe from Fig. 2b–2c that the flat CFCs of the fourth TM band extend almost over the entire frequency range of the fourth band, thus enabling super-collimation over a significant frequency range. Moreover, except near the edges of the fourth band, the CFCs are flat for all the values of $k_y$ and not just in the vicinity of $k_y = 0$. This last feature indicates that our proposed structure can support super-collimation of spatially narrow beams. Note that the flattest CFC for the structure with $r = 0.16a$ and $t = 0.2a$, has angular frequency $\omega = 0.495(2\pi c/a)$.

Having found the optimum parameters for our proposed structure, we study the propagation of a beam with Gaussian envelope and angular frequency $0.495(2\pi c/a)$, along the $x$-direction, in one of the waveguides of our optimum structure. We represent the $z$-component of the electric field of such a beam as

$$E_z(x, y; t) = e^{-i\omega t} \int_{\substack{k_y \text{ values on} \\ \text{CFC of freq. } \omega}} dk_y \, e^{-(k_y)^2/2(\sigma_{k_y})^2} E_{(k_x, k_y)}^{n=4}(x, y) \equiv e^{-i\omega t} A(x, y) \quad (2)$$

where $E_{(k_x, k_y)}^{n=4}(x, y)$ is the E-field of the TM Bloch modes on the CFC with $\omega = 0.495(2\pi c/a)$. We define the diffraction length $L_{\text{diff}}$ as the distance in the $x$-direction that the beam propagates before the full-width at half-maximum (FWHM) of $|A(x, y)|^2$ spreads by a factor of $\sqrt{2}$ from its initial value at $x = 0$. For $\sigma_{k_y} = 0.12(2\pi/a)$, the beam is localized mostly in 3 waveguides only, as shown in Fig. 3a, and the diffraction length is $L_{\text{diff}} = 500a$. To obtain an
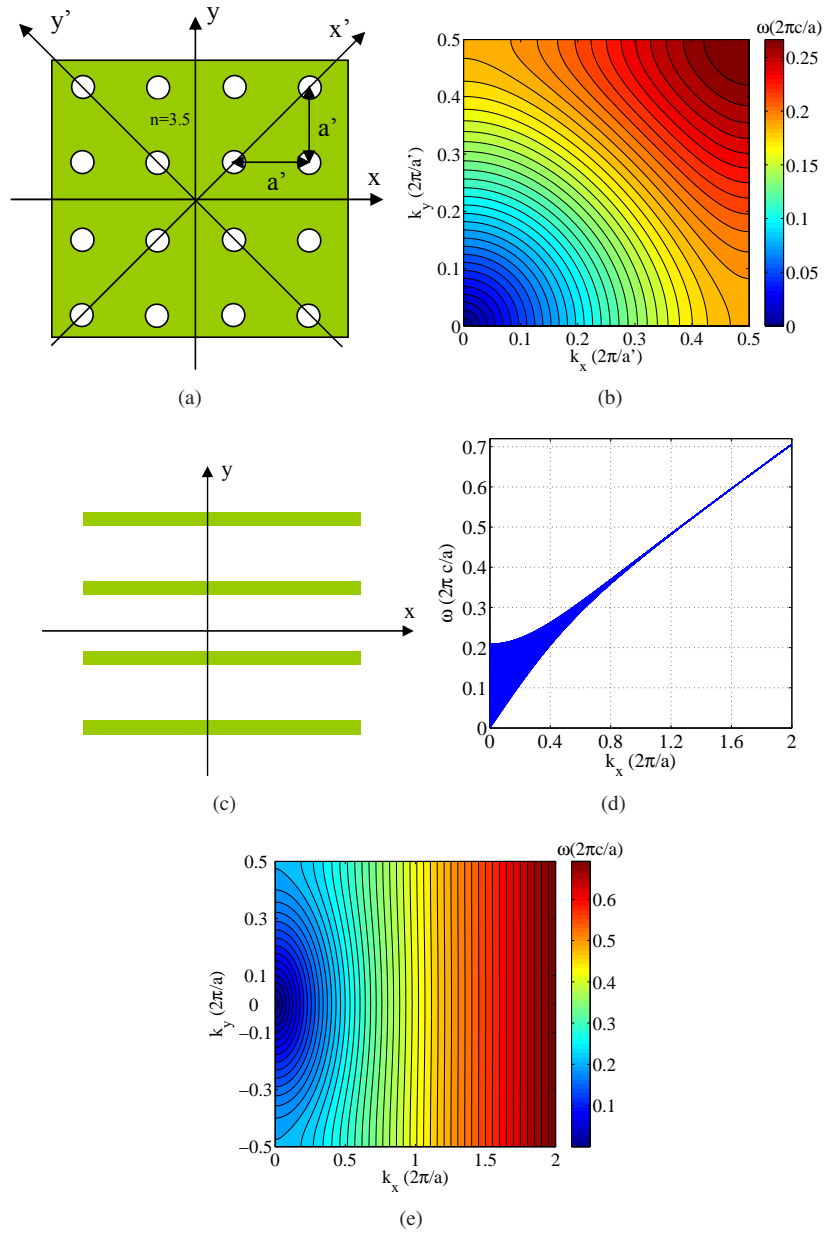
Fig. 1. (Color online) Two "often-used" low-diffraction structures. (a) Profile of the refractive index of a 2D holes-in-dielectric structure, with the dielectric having $n = 3.5$, and the holes having radius $r = 0.421a'$, where $a'$ is the nearest-neighbor center-to-center separation between holes (the square lattice spacing). Note that the holes form a square lattice. (b) Color contour plot of the frequency of the first TE band for the structure shown in Fig. 1a. (c) Profile of the refractive index for a waveguide array structure, with the waveguide having refractive index $n = 3.5$. (d) Projected band diagram of the first TM band for the waveguide array with $t = 0.2a$. (e) Color contour plot of the frequency of the first TM band for the waveguide array with $t = 0.2a$.

estimate of the operational frequency width over which the CFCs are flat enough to support super-collimation, we define the frequency bandwidth $B_{k_x}$ at a particular $k_x$ by the expression $B_{k_x} = \max_{k_y}[(\omega_4(k_x, k_y)] - \min_{k_y}[(\omega_4(k_x, k_y)]$. A small value of $B_{k_x}$ for a certain $k_x$ means that the $\omega_4$'s for all values of $k_y$ (for the particular $k_x$ in question) are of a similar value; $B_{k_x}$ is hence a measure of the "band flatness" at a given $k_x$ value. The $k_x$-value that minimizes $|\alpha_4^{TM}(k_x)|$ is $0.25(2\pi/a)$, and the frequency bandwidth there is $B_{k_x} = 0.0008(2\pi c/a)$; the CFC associated with the minimum of $|\alpha_4^{TM}|$ has $\omega = 0.495(2\pi c/a)$. Next, we ask over which frequency range does $B_{k_x}$ not change appreciably, to obtain a measure of the frequency range over which our structure supports super-collimation. $B_{k_x}$ remains below $0.0008\sqrt{2}(2\pi c/a)$ in a frequency range from $0.493(2\pi c/a)$ to $0.558(2\pi c/a)$. Hence, the relative frequency range over which our optimum structure supports super-collimation is $(0.558 - 0.493)/0.495 = 0.13$, or 13%.
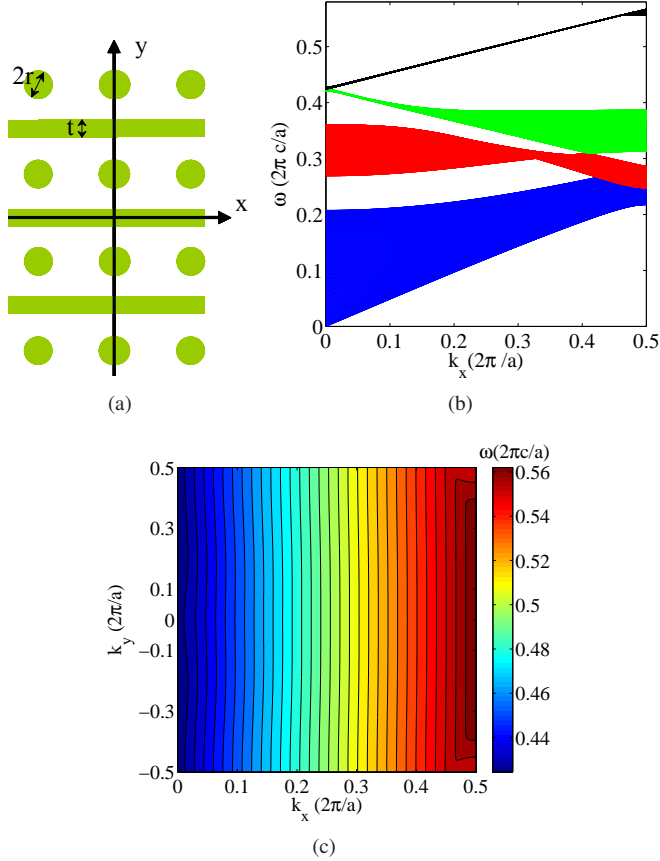


(a)          (b)



(c)

Fig. 2. (Color online) Proposed 2D PhC structure (a) Schematic of the refractive index: the rods, of radius $r$, and waveguides, of thickness $t$, (shown in green) both have $n = 3.5$, and are surrounded by air ($n = 1$). The rods form a square lattice, with lattice constant $a$, and the waveguides are halfway (on the $y$-axis) between the rods. (b) Projected band diagram of lowest four TM bands for $r = 0.16a$ and $t = 0.2a$. (c) Color contour plot of the frequency of the fourth TM band.

## 3. Super-collimation mechanism in other structures

### 3.1. Holes-in-dielectric structure

Having explored super-collimation in our structure proposed in Fig. 2a, we now study super-collimation in the two other previously-mentioned structures. We first start with the 2D holes-in-dielectric structure shown in Fig. 1a and take the refractive index of the dielectric to be $n = 3.5$. Super-collimation was demonstrated in this structure[13], for a beam propagating along the $x'$-direction (diagonal), at the frequency of the flattest CFC of the first TE band. Because of the structure's mirror symmetry with respect to the plane $y' = 0$, we expand the angular frequency close to the super-collimation frequency in even powers of $k_{y'}$

$$\omega_1^{TE}(k_{x'}, k_{y'}) = \omega_1^{TE}(k_{x'}, 0) + \alpha_1^{TE}(k_{x'}) \cdot (k_{y'})^2 + \beta_1^{TE}(k_{x'}) \cdot (k_{y'})^4 + \dots \qquad (3)$$

Since the frequency range in which we have super-collimation is known to be small in this structure, we consider maximizing the propagation length at the super-collimation frequency, instead of maximizing the frequency bandwidth around it (as we did for the structure proposed in Fig. 2). In order for this structure to support super-collimation over the longest propagation length, the holes' radius $r'$ needs to be chosen such that $\omega_1^{TE}(k_{x'}, k_{y'})$ depends very little on $k_{y'}$. It is known from Ref.13 that there always exists a value of $k_{x'}$ at which $\alpha_1^{TE}$ is zero since it changes sign from negative to positive. We denote this value by $k_{x'}^o$, so that we have $\alpha(k_{x'}^o) = 0$. Therefore, to minimize the dependence of $\omega_1^{TE}(k_{x'}, k_{y'})$ on $k_{y'}$, we searched for the radius $r'$ that minimizes $|\beta(k_{x'}^o)|$, and found that $r' = 0.421a'$ where $a'$ is the lattice constant of the holes' structure, along the $x$ and $y$ directions. A color contour plot of the first TE band for this optimum hole radius was obtained by using MPB, and is shown in Fig. 1b. The minimum frequency bandwidth occurs at the value of $k_{x'}$ corresponding to $\omega(k_{x'}, k_{y'} = 0) = 0.1966(2\pi c/a')$, and has a value of $B_{min} = 0.0034(2\pi c/a')$. It spreads by a factor of $\sqrt{2}$ at $k_{x'}$-values with maximum frequencies equal to $0.1945(2\pi c/a')$ and $0.2004(2\pi c/a')$. Hence, the relative frequency range over which the optimum 2D holes structure supports super-collimation is 0.03 (or 3%), which is smaller than that of our proposed structure by a factor of 4.3. The minimum value (over $k_{x'}^o$) of $|\beta_1^{TE}(k_{x'}^o)|$ for the optimum 2D holes structure having $r' = 0.421a'$, occurs at $k_{x'}^o = 0.457(2\pi/a')$, where we have $\omega_1^{TE}(k_{x'}^o, k_{y'} = 0) = 0.2124(2\pi c/a')$. Thus, we calculate the diffraction length of a beam with gaussian envelope and angular frequency $0.2124(2\pi c/a')$ propagating along the $x'$ direction in the optimum 2D holes-in-dielectric structure. If we set the physical frequency of this beam to be the same as that for the optimum structure in Fig. 2, then the lattice constant $a'$ in the holes' structure is related to that in Fig. 2 by $a' = (0.2124/0.495)a$. In this case, sending a beam of the same physical width as before corresponds to using $\sigma_{k_{y'}} = 0.12 \times (0.2124/0.495)(2\pi/a')$, and yields a diffraction length of $707a' = 303.4a$. So the collimation length in this optimum 2D holes-in-dielectric structure is shorter than that in our proposed structure by a factor of 1.65, when we use beams of the same physical frequency and same physical width. We show in Fig. 3b how such a beam spreads after it propagates, along the diagonal of the optimum 2D holes structure, a physical distance equal to the collimation length ($500a$) of our proposed structure.

### 3.2. Waveguide arrays

Now we explore how the super-collimation mechanism in our proposed structure compares to that in the waveguide array structure, shown in Fig. 1c. Again, we set the refractive index of the waveguides to $n = 3.5$, and we consider the first TM band. The reason for which we deal with the first TM band in this case, is that the physical k-point of interest (with angular frequency $\sim 0.4952\pi c/a$) now lies in the first TM band. We first study the waveguide array structure having waveguide thickness $t = 0.2a$. This structure is the same as our proposed structure, but
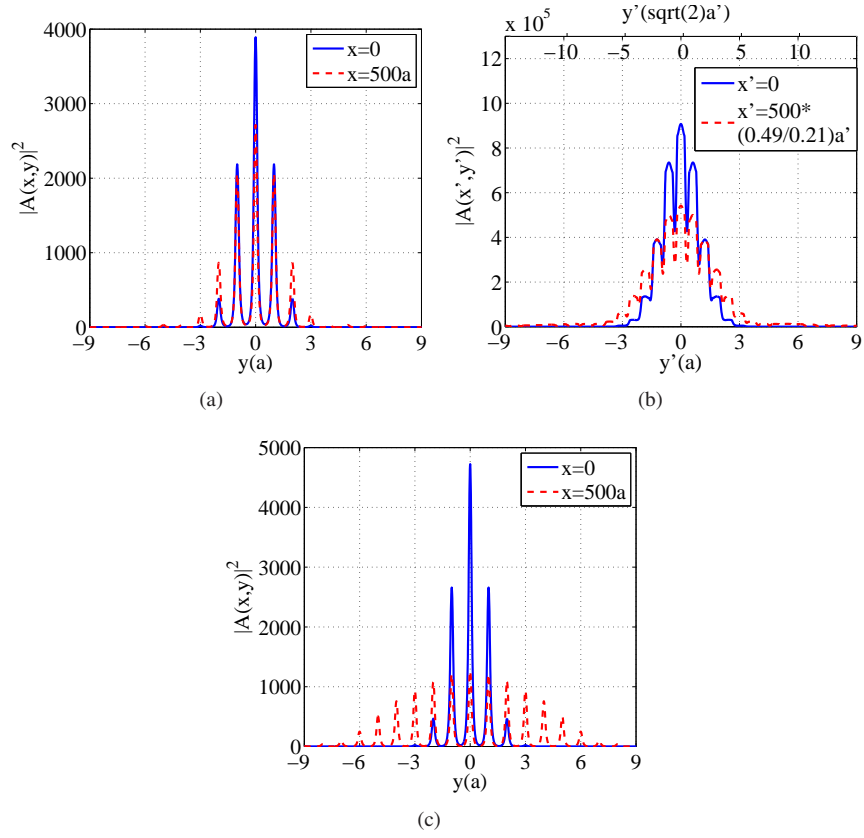
Fig. 3. (Color online) Intensity profile of the propagating beam (of angular frequency $0.495(2\pi c/a)$, and physical width corresponding to $\sigma_{k_y} = 0.12(2\pi/a)$) as a function of $y(a)$, at $x = 0$ (in blue) and at $x = 500a$ (in red), in (a) Our proposed PhC structure shown in Fig. 2, (b) The 2D holes structure shown in Fig. 1a, but with lattice constant $a' = (0.2124/0.495)a$, where $a$ is the lattice constant in our proposed structure and in the waveguide array structures, (c) The waveguide array structure with $t = 0.2a$. Note that the spikes in (a) and (c) correspond to the positions of the "waveguide" strips.

with the rods removed. In Fig. 1d, we show a projected band diagram of the first TM band, and in Fig. 1e we show a color contour plot of the first TM band. We note from these last two figures that the CFCs get flatter as the frequency increases (i.e. as $k_x$ increases). This is a consequence of the fact that, as the frequency is increased, the modes tend to be more concentrated into the waveguides, and hence the overlaps between neighboring waveguides modes become weaker and result in narrower frequency bandwidths $B_{k_x}$. Note that because of the continuous translational symmetry along $x$, the value of $k_x$ ranges from 0 to $\infty$, whereas the values of $k_y$ range only between $-0.5(2\pi/a)$ and $0.5(2\pi/a)$ due to the discrete translational symmetry in the $y$-direction. Sending a beam of the same physical angular frequency $0.495(2\pi c/a)$ and same physical width $\sigma_{k_y} = 0.12(2\pi/a)$ as in the structure of Fig. 2, we get a collimation length of $160a$, which is shorter than that of our proposed structure by a factor of 3.125. In Fig. 3c, we show how significantly this beam spreads after it has propagated a distance of $500a$, i.e. after it has propagated by a distance equal to the collimation length in Fig. 2.

One might argue that the sole role that the rods were playing in our structure was to merely increase the effective index of refraction, and therefore to push the flat CFCs to lower frequencies. To show that this is not the case, we considered a waveguide array structure having the same effective index as our proposed structure in Fig. 2, namely we chose the waveguide thickness to be $t' = t + \pi r^2 = [0.2 + \pi(0.16)^2]a = 0.28a$. We then launched a beam of the same physical frequency $0.495(2\pi c/a)$ and the same physical width as before, and we obtained a collimation length of $275a$, which is shorter than the collimation length of Fig. 2, by a factor of 1.8. So the rods play a more important role in our proposed structure than just increasing the effective index. In fact, the rods break the continuous translational symmetry along the waveguide direction, and as in the holes-in-dielectric structure[13], the discrete translational symmetry along $x$ results in a change of sign of the concavity somewhere in the interior of the flat band. Due to this change in the sign of the concavity, there exists a value of $k_x$ where the concavity is zero and the associated CFC is superflat. However, in the waveguide array case, the concavity never changes sign because of the continuous translational symmetry along $x$. And therefore, the leading deviation of $\omega(k_x, k_y)$ from $\omega(k_x, 0)$, in the waveguide array case is expected to be larger than that in our proposed structure. This accounts for the longer collimation length in our proposed structure, for beams of the same physical frequency and same physical width.

## 4. Conclusion

In conclusion, we proposed a PhC structure that exhibits long-scale super-collimation over a large frequency range. We compared the super-collimation phenomenon exhibited by our proposed structure to that in two other often used related structures. We have shown that our structure supports super-collimation over longer propagation lengths than waveguide arrays and 2D holes-in-dielectric PhCs, due to the different translational symmetries involved in each structure type. Moreover, the operational frequency range over which our structure exhibits super-collimation is 4 times larger than in the 2D holes case. These two features make our proposed structure of importance in the design of super-collimation-based devices. In particular, the large operational frequency range of our proposed structure suggests the possibility of achieving super-collimation of polychromatic beams. In addition to super-collimation, our proposed structure exhibits negative refraction[5], since the group velocities of modes in the second and third TM bands, point opposite to the phase velocities. Moreover, beam steering[19] is possible in our structure as well, due to the sharp corners in the CFCs of the second and third bands. Finally, we note that our structure could be used for directional thermal emission[8], because the group velocities of most of the modes in its fourth TM band point in the same direction. We leave detailed investigations of these possibilities as future work.

**Acknowledgements**